Measurement of the pyroelectric coefficient of poly(vinylidene fluoride) down to 3 K

R. W. Newsome, Jr. and E. Y. Andrei
Department of Physics and Astronomy, Rutgers University, Piscataway, New Jersey 08855
(Received 6 September 1996; revised manuscript received 22 November 1996)

The temperature dependence of the pyroelectric coefficient p' of polyvinylidene fluoride (PVF_2) was measured from 307 K to the previously unexplored region of 3 K. The measurements were performed on a film of oriented (β-phase) PVF_2 by monitoring its surface charge response to quasistatic heating and cooling transients. The data exhibit a pure cubic temperature dependence from 3 to 6 K with no evidence of a linear term. This is consistent with the prediction by Szigeti and the Debye limit, respectively, for the primary (i.e., strain-free) and secondary contributions to pyroelectricity. The data from ~20 to ~150 K, which include the region of largest change, are well fit by an exponential function (i.e., $a_0 e^{-\theta/T}$), corresponding to a thermal activation energy of $\theta=(25.9\pm0.06)$ K. Our data for p', from 100 to 250 K, are approximately proportional to the thermal expansion coefficient, recently published by Hartwig, which indicates that the observed pyroelectricity is dominated by piezoelectric (i.e., secondary) contributions in that temperature regime. [S0163-1829(97)08211-8]

I. INTRODUCTION

A. Overview

Most studies of the pyroelectric coefficient of polyvinylidene fluoride (i.e., PVF_2 or PVDF) have focused on the temperature regime above the primary glass transition at ~200 K, where the coefficient is comparatively large. There are no previously reported measurements of it below 10 K for PVDF,[1–4] or for its related copolymer with trifluorethylene, P(VDF-TrFE).[5,6] Predictions by phenomenological models for idealized crystals have differed, historically, between a linear[7–9] and a cubic[10–13] temperature dependence for the primary (i.e., strain free) component of the pyroelectric coefficient in the low-temperature Debye limit.

Our measurements of the pyroelectric coefficient, defined as $p'=(1/A)(\partial Q/\partial T)$, of oriented ($\beta$-phase) PVF_2 extend from 3 to 307 K. The change in charge ΔQ on the sample surface of area A was measured in response to a change in the temperature ΔT under conditions of negligible external mechanical stress and electric fields. The temperature regime below 20 K received special emphasis because previous measurements there are sparse and qualitative.[1–6] The measurements presented here provide evidence of a pure cubic temperature dependence of p' from 3 to 6 K. There is a break in the slope of p' at 6 K, and the data show evidence of quadratic and linear temperature-dependent terms in the transition region from ~6 to ~20 K. From ~20 to ~150 K, the data are readily fit by an exponential $a_0 e^{-\theta/T}$, typical of thermal activation over a barrier, with $\theta=25.9$ K.[14] In the vicinity of the primary glass transition region at ~200 K, the magnitude of p' shows evidence of thermally driven hysteresis.

There are many articles which review the properties and applications of PVF_2.[15–18] This polymer was first fabricated as a functional ferroelectric in 1969.[19] The fast response and small thermal mass of thin films of PVF_2 make them increasingly popular as sensors in various applications such as photopyroelectric spectroscopy, as differential thermometers in calorimetry, and for measurements of thermal diffusion. The extended range and improved accuracy of our data may aid in their evaluation for such roles.

B. Background and definitions

Symmetry constraints for pyroelectric phenomena associate them with a specific direction in space, and they can only occur in noncentrosymmetric crystals.[20,21] When there is no external electric field, the pyroelectric coefficient is defined as the change in the bulk polarization in response to a temperature change, typically performed under conditions of no external mechanical stress. The bulk polarization **P** is represented classically as a macroscopic manifestation of mean-field effects due to residual electric-dipole moments.[20,21] Discontinuities at the sample boundaries create a surface charge density $\sigma=P_3$, where P_3 is the component of polarization normal to the surface. This surface charge is rapidly neutralized by stray charges in the external environment. Although this classical model provides a useful framework for the phenomenological theories referred to here, its utility does not extend to ongoing efforts, focused on systems simpler than PVF_2, to predict residual polarization from *ab initio* quantum-mechanical calculations based on microscopic properties.[22]

An equivalent expression for our measured quantity is obtained by expanding the thermodynamic equation of state (i.e., the Gibbs free energy)[20,21,23]

$$|p'| \equiv \frac{1}{A}\left(\frac{\partial Q}{\partial T}\right)_{\boldsymbol{\Sigma},\vec{\mathbf{E}}=0} = \left(\frac{\partial P_3}{\partial T}\right)_{\eta,\vec{\mathbf{E}}=0} + d_{3jk}c_{jklm}\alpha_{lm} + P_3\alpha_A . \qquad (1)$$

The left side of this equation defines the magnitude of p' under conditions of no external mechanical stress $\boldsymbol{\Sigma}$ or electric fields **E**. The first term on the right is the primary pyroelectric coefficient p_I. It represents the thermal response of P_3 under conditions of no strain, η (i.e., fixed macroscopic

dimensions). The second term on the right represents the secondary or piezoelectric contributions p_{II}. It is due to thermally induced changes in macroscopic dimensions, and consists of a product of the direct piezoelectric coefficient **d**, the elastic stiffness tensor **c**, and the thermal-expansion coefficient α. The third term, which contains the two-dimensional thermal-expansion coefficient $\alpha_A=\alpha_1+\alpha_2$, where α_1 and α_2 are the coefficients along principal axes of the surface, is a correction[21,23,24] which arises because we measure the surface charge and not the surface charge density.

Several theoretical models of pyroelectricity have dealt with the low-temperature behavior of p_I.[7–13] One of the early models, developed by Born, used an acoustic-phonon representation[7] to predict a linear temperature dependence for p_I in the Debye limit. A subsequent version,[10] based on the assumption that the anharmonic term in the potential appears only in p_{II}, predicted a cubic temperature dependence, which is consistent with measurements[25] of p' down to 10 K for a crystal of ZnO. A cubic temperature dependence was also predicted when the Born model was subsequently extended to include contributions to p_I from the anharmonic potential term as well as the second-order moment,[11,12] arising from deformations of the electron clouds. Neither of these models include possible effects due to the long-range order associated with ferroelectricity. They may become significant near the Curie point, which occurs in PVF_2 at about 20 K above its melting point of 448 K,[15] but they should be negligible at the temperatures of our measurements.

A mean-field molecular theory was alternatively used[8,9] to predict a linear low-temperature dependence for p_I in substances with large values of p', on the premise that the latter implies large deformations of the electron clouds. But thermodynamical arguments were used to exclude this possibility in substances where p_I is negative.[13] Specifically, the claim is that a negative p_I cannot have a temperature dependence which decreases slower than that of the specific heat at constant volume, without the contradictory inference of a decrease in entropy as the temperature approaches absolute zero. Several measurements have confirmed that the sign of p_I is negative for PVF_2 in the vicinity of room temperature.[15,16] Related measurements on the copolymer show no evidence of a sign change at low temperature.[5]

Since our experiments give a global measure of p', and provide no direct information about p_I, comparison to theoretical models can be made only by making certain assumptions about the remaining terms.

The temperature dependence of the second term p_{II} can be estimated by noting that it is dominated by α, because the multiplicative compliance coefficients are typically constant at very low temperatures. Since α is related to the specific heat by the Grüneisen factor γ, one expects $p_{II}\propto T^3$ in the Debye limit, if γ is constant there.[26]

To estimate the contribution from the third term, we note that related measurements on the copolymer[5] indicate that P_3 is proportional to p' from 10 K to room temperature. If we assume that this property is unchanged in the stretched version of the material, i.e., that P_3 and p' have the same temperature dependence down to low temperatures, then the third term should have the same temperature dependence as $p'\alpha$. Our low-temperature data show $p'\propto T^3$ below ~ 6 K, and exhibits quadratic and linear temperature-dependent terms in the transition region from ~ 6 to ~ 23 K. If α has the typical T^3 dependence below the effective Debye temperature, estimated to be well above 20 K,[26,27] then these results also imply that the third term in Eq. (1) has a T^4 dependence, or greater, for temperatures below 20 K. As the observed temperature dependence is T^3 or less, we conclude that the third term contribution is negligible. This contribution is not negligible at room temperature, however, where it is estimated to be $\sim 25\%$. Nevertheless, no correction was applied to our higher-temperature measurements, because of the limited temperature range and accuracy of available data for the bulk polarization and thermal-expansion coefficients. This convention also facilitates direct comparisons with other reported measurements of p', which are customarily presented in this way.

Our data are also not corrected for the temperature dependence of the area normalization factor $(1/A)$. That correction was neglected as it is only $\sim 3\%$ over the temperature range from 24 to 250 K.[26,28]

The possibility of a fourth contributor was suggested because individually resolved measurements of p_I and p_{II} fell short by $\sim 35\%$ of the independently measured value of p' at room temperature.[16,29] Reversible phase changes in the volume amount of crystallinity were proposed to explain this short fall,[16,29,30] but a theoretical model of this phenomenon yields results that are much too large.[31] It was then postulated that the discrepancy may be due to reversible disordering of dipoles associated with strain throughout the volume of the sample.[32] This would be another form of secondary pyroelectricity, and would also depend on the thermal-expansion coefficient. Uncertainty still exists as to the relative importance of these contributors to pyroelectricity, and this issue cannot be resolved by our data.

Our data show a ''pure'' T^3 temperature dependence for p' below 6 K. This is significant because measurements of the temperature dependence of p' become increasingly sensitive to T^1 compared to T^3 terms as the temperature decreases below the Debye value. On the basis of the previous discussion, we conclude that the first and second terms in Eq. (1), i.e., p_I and p_{II}, are the primary source of this temperature dependence of p', however, our measurements cannot resolve their relative contributions.

II. MEASUREMENT AND CALIBRATION PROCEDURES

A. Sample and apparatus

The polymer PVF_2 consists of long chains of the molecular monomer CH_2CF_2, where the hydrogen and fluorine atoms are offset from the backbone of the carbon chain. The oriented β phase of the polymer has two parallel dipoles per unit cell, and it retains a residual polarization after it is mechanically stretched and then poled by a strong electric field at elevated temperature. The strong polar bond between the fluorine and carbon atoms can account for approximately 50% of the bulk polarization of PVF_2 at room temperature. The dipole strength of a monomer unit of PVF_2 is 2.1 D, or equivalently, 7.0×10^{-30} C m, obtained by adding the dipole moments of $+1.39$ and -0.29 D, respectively, for the covalent bonds of C-F and C-H.[15,18] Estimates based on the orthorhombic cell dimensions of 8.58, 4.91, and 2.56 Å for sides

a, b, and c, respectively, lead to a polarization density per unit cell of 0.13 C/m^2, which is surprisingly close to the measured value.[15,18] At room temperature, approximately 50% by weight of these chains crystallize into lamellar domains that radiate out from ball-shaped clusters known as spherulites, which reside in an amorphous matrix of tangled chains.

The PVF_2 sample in these experiments was an oriented, β-phase film obtained from ATOCHEM/AMP, Inc. This phase was created by mechanically stretching the material by a factor of approximately 5, in order to align the molecular chains. The residual polarization was then induced by applying a poling field, oriented perpendicular to the surface. The polar β phase can also be created via a mixture of two polymers that form a copolymer, which avoids the need for mechanical stretching.[5,6,15] The linear expansion coefficients for the stretched sample at room temperature, are $\alpha_1 = 0.13 \times 10^{-4}\ K^{-1}$ and $\alpha_2 = 1.45 \times 10^{-4}\ K^{-1}$, where the subscripts refer to directions in the plane of the surface which are respectively parallel and perpendicular to the draw direction.[29] Both surfaces of the film were coated with a $\sim$340-Å-thick layer of NiCu to facilitate detection of induced charge.

The sample was 6 mm in diameter and 9μ thick. It was mounted vertically, with a thin layer of vacuum grease, onto an alumina substrate, of 0.038-cm thickness. The substrate was glued with epoxy to the inner surface of a copper box which served as a high conductance heat reservoir and as an electrical shield. Electrical leads of maganin wire were connected to the PVF_2 film with silver paint. The charge on the film was monitored with a Keithley 617 electrometer. The preamplifier of the electrometer has a negative feedback loop which creates an effective capacitance much larger than that of the film. Charge is therefore efficiently swept off the film electrodes, which reduces external electric fields to negligible values.[21] The temperature of the substrate was monitored with an encapsulated silicon diode. This thermometer was attached to the alumina substrate with a thin layer of General Electric GE-7031 varnish. It was calibrated below 90 K by direct comparison with readings from a precision-calibrated resistor when both were cooled over a range extending down to a few degrees below that of liquid helium. A least-squares fit of a sixth-order polynomial to the calibration data points yielded a curve of voltage versus temperature whose slope was smooth and slowly varying except in the region of the $\sim$25-K knee, which was avoided in the data analysis.

The copper container was mounted at the end of a sealed, stainless-steel tube which could be readily raised or lowered into a column of liquid helium. The sample holder was open at one end to facilitate equilibrium with the helium heat-exchange gas. A resistive heater, located between the helium reservoir and the sample holder, was used to initiate quasistatic variations in temperature above that of the reservoir. Heating and cooling runs were alternated for temperatures below 30 K. Each run lasted from 40 to 60 s, and the electrometer was discharged after each run. At higher temperatures, where thermal time constants are larger, the heating and cooling runs were grouped in bunches of each kind, in order to minimize start-up transients in temperature.

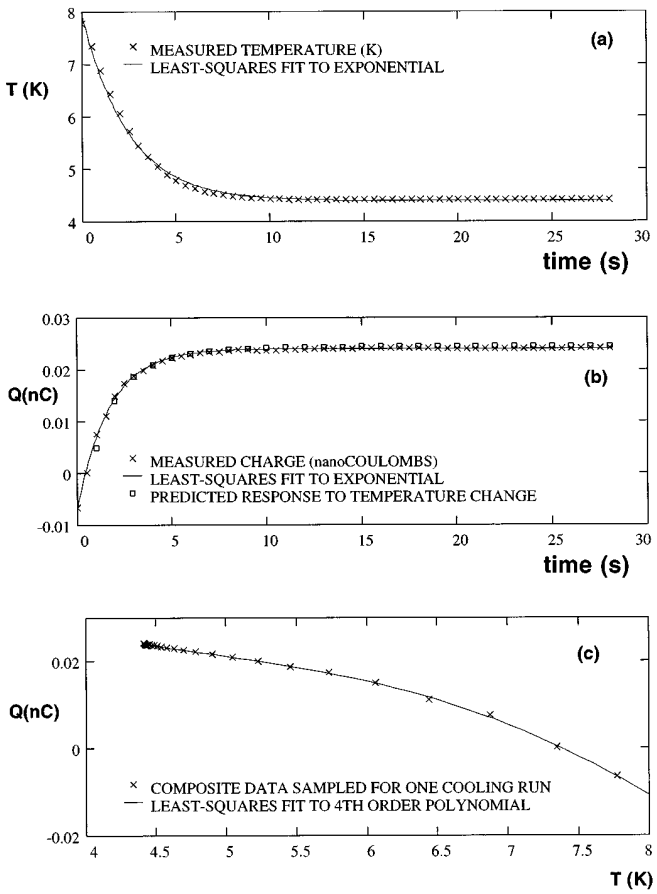

FIG. 1. A typical cooling run, showing the thermal (a) and charge (b) responses of the PVF_2 film near the temperature of liquid helium. The predicted charge response in (b), is the product of the sample area A, and the integral of the measured p' over the temperature interval. The measured charge is plotted as a function of temperature in (c).

B. Measurement procedures

Our measurements of p' consist of monitoring the sample response to a heating (or cooling) pulse which is produced by changing the power into the heater. In parts (a) and (b) of Fig. 1 we show the time evolution of both temperature and sample charge obtained in a cooling run to $\sim$4 K which was initiated by disconnecting the heater. The same data are redrawn in Fig. 1(c) with the time axis suppressed to show the temperature dependence of the charge $Q(T)$. The slope of the $Q(T)$ curve represents the absolute value of the pyroelectric coefficient $|p'|$. This slope was obtained[33] via straight-line approximations over temperature intervals of about 0.5 K. The slopes were also calculated by taking the derivative of the analytical expression obtained from a fourth-order polynomial fit to the data shown in Fig. 1(c). That method has the advantage of giving $p'(T)$ without averaging over a finite-temperature window. There was no significant difference, in either the averages or their scatter, for the data processed by the two methods.

One of the pitfalls in measurements based on thermal transients is the production of spurious signals from thermal gradients. Such gradients may create local changes in crystalline symmetry that can cause tertiary contributions to the pyroelectric response.[20,34] The thin layer of vacuum grease is

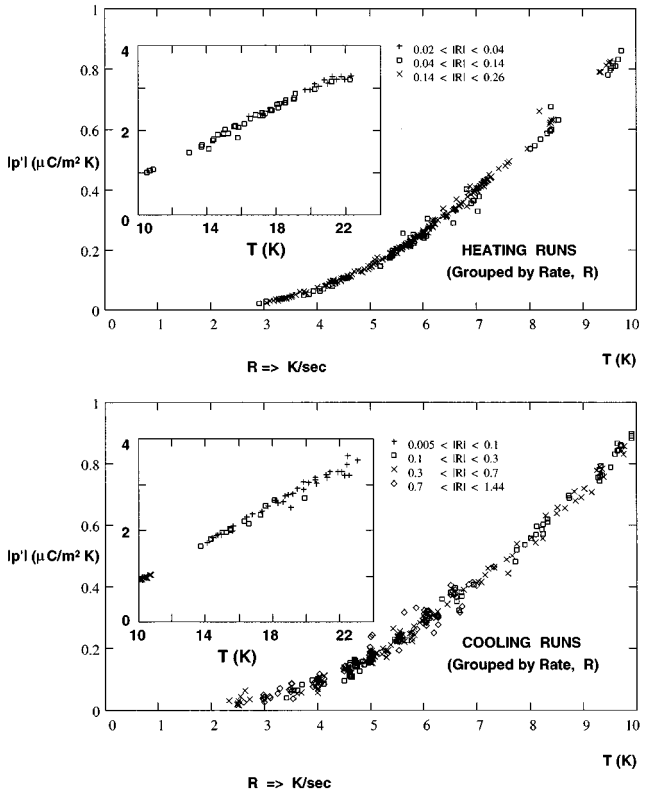

FIG. 2. Plots of the raw data from 3 to 10 K, with inserts from 10 to 23 K, grouped to display rate effects.

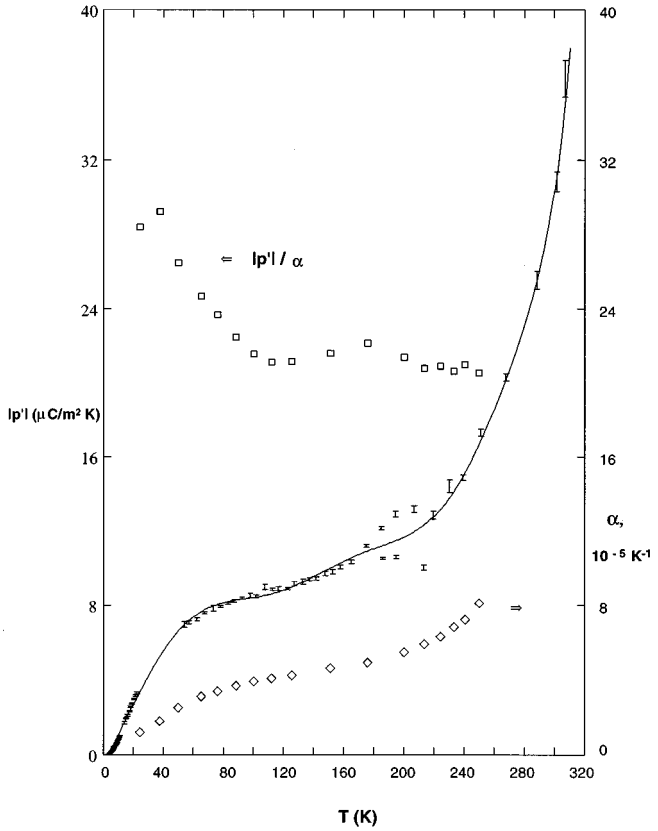

FIG. 3. Temperature dependence of the pyroelectric coefficient $|p'|$ of PVF_2, averaged over all heating and cooling runs, and compared with the thermal expansion coefficient, α (Ref. 26), whose data points are represented by the symbol $\diamond$. The length of each vertical error bar bounds the region of $\pm\overline{\sigma}$, where $\overline{\sigma}$ represents the root-mean-square standard deviation of the mean of approximately equal numbers of heating and cooling runs. The solid curve represents the least-squares fit of a ninth-order polynomial to the raw data. The $\square$ symbols represent the ratio $|p'|/\alpha$, plotted with an arbitrary scaling factor.

a potential source of gradients in temperature and mechanical stress, because it may clamp the bottom of the film to the substrate when it freezes.[35–37] There is, however, independent evidence from measurements on an unstretched copolymer, that surface clamping is not effective at temperatures well below the glass transition, due to the increased stiffness of the elastic compliance factors.[36] This is likely to be the case for our samples also, since the piezoelectric strain coefficients for our stretched polymer are similar to those for the copolymer.[36,38] Data for the thermal expansion coefficient of PVF_2 show that most of the stress due to thermally induced strain occurs above 150 K.[26]

Thermal gradients in the sample often produce rate effects. The absence of rate-dependent biases in the data is therefore a good indication of thermal equilibrium. There is no evidence of such effects in the extensive collection of raw data for p' displayed in Fig. 2, which are sorted over a wide range of heating and cooling rates. The comparatively low background signal, observed at quiescent temperatures, is also consistent with the absence of unrelieved strain in the sample.

The temperature dependence of $|p'|$, over the entire range of our measurements, is presented in Fig. 3. The data was obtained by averaging many heating and cooling runs over small temperature intervals. The combination of heating and cooling runs is important because the sign of the induced charge reverses for pyroelectric effects but not for most other sources of background, such as thermally stimulated discharge of trapped charge and triboelectric charging due to friction and differences in contact potentials.[39,40] Therefore an equally weighted average of the magnitudes of heating and cooling runs was used to cancel the first-order effects of background due to unidirectional charging.

The response of our PVF_2 sample to a sinusoidal heat source is shown in Fig. 4. These data provide an alternative evaluation of the relative contributions from pyroelectric and thermally stimulated sources of current, because the former are out of phase with the thermal source, whereas the latter are in phase with it.[41] Specifically, the current associated with pyroelectricity is proportional to the time derivative of the temperature, $i_p = p'A(dT/dt)$, and therefore, pyroelectric currents should be out of phase with the temperature as well as most spurious modulations. Harmonic analysis of the charge and temperature response to the sinusoidal voltage of frequency $f = 0.05$ Hz, plotted in Fig. 4, confirm the absence of in-phase contributions to the charge current, measured at an average temperature of ~ 5.5 K. The ratio of the $2f$ component of the charge and temperature response, normalized by the sensor area A, yields a value for $|p'|$ in good agreement with our other measurements at this temperature, summarized in Fig. 2.

III. DATA PRESENTATION

A. Overview from 3 to 307 K

The comprehensive summary of our data for p' in Fig. 3 is generally consistent with reports from recent measurements at temperatures above ~180 K.[1–6,42,43] In addition, our data indicate the possible existence of temperature-dependent hysteresis in the glass transition region at ~200 K. For example, rapid cooling of the cryostat yielded data points only along the upper branch of the apparent double-valued region for $|p'|$ in the vicinity of 200 K, as plotted in Fig. 3. The associated peak in $|p'|$ observed in this region may be due to internal stress caused by differences between the thermal-expansion coefficients for the amorphous and crystalline components of PVF_2.[44]

Our data in Fig. 3 are compared with recently published values for the linear expansion coefficient in PVF_2.[26] If the last two terms in Eq. (1) were dominant at intermediate temperatures, then p' would have the same temperature dependence as α, if their multiplicative coefficients were constant. The ratio p'/α is indeed comparatively flat from about 100 K to ~250 K. This result is consistent with previous claims that p_{II} dominates at higher temperatures. Below 100 K, p'/α deviates significantly from the constant value. Similar results were obtained in radiant heating (laser) measurements,[3] which are sensitive to the ratio p'/c_p, and by direct comparisons of extrapolated values for c_p.[27] In all cases, however, there is an obvious need for more extensive and accurate measurement of α, and of c_p, at temperatures below 20 K.

B. Intermediate-temperature range from 10 to 150 K

The data in Fig. 5 are well fit over the 20–150-K range by, $(a_o)e^{-\theta/T}$, with $\theta=(25.9\pm0.06)$ K, indicating a thermally activated process.[14] Note that the least-squares fit is not to the composite averages, but to the individual data for each of the heating and cooling runs from which these grouped averages were deduced. The data points outside the interval from ~20 to ~150 K, show small but consistent deviations from the fitted line in Fig. 5.

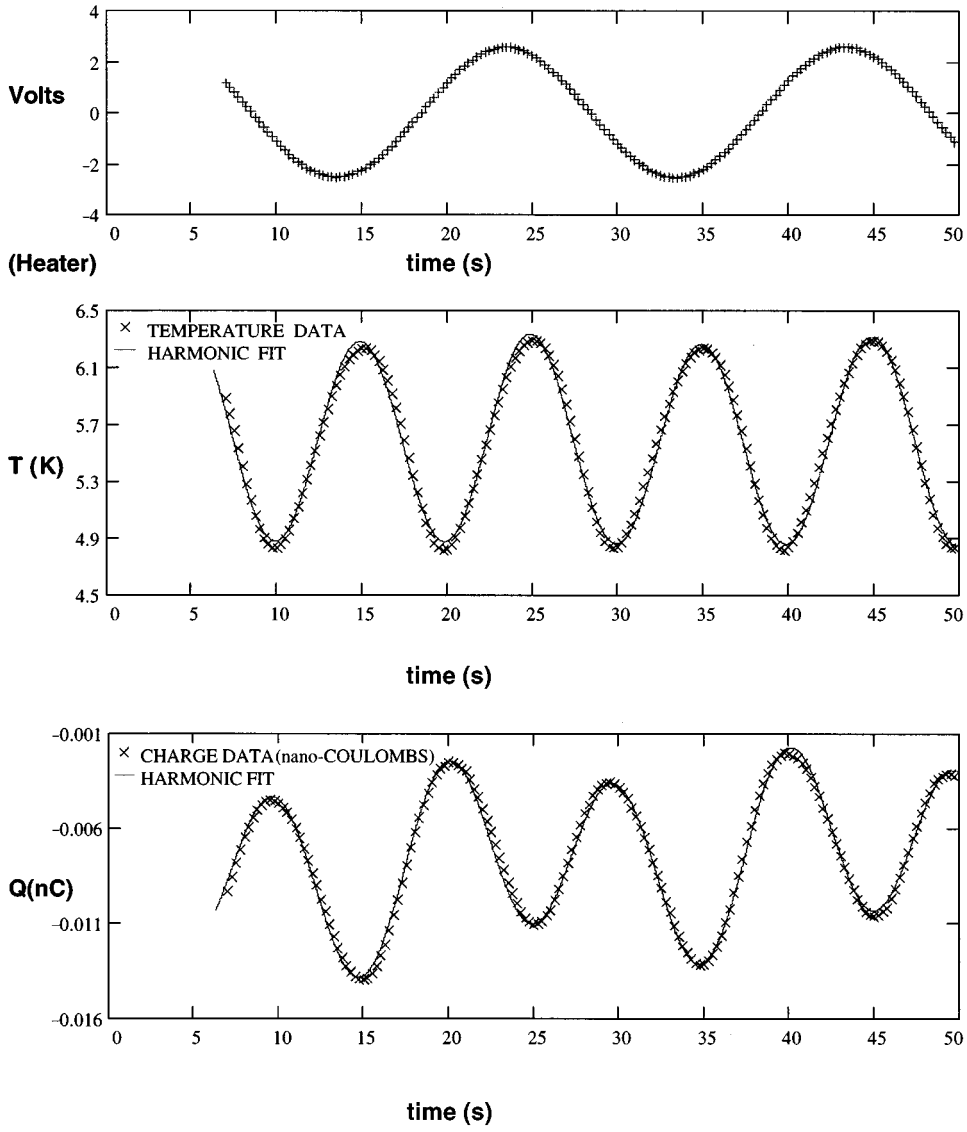

FIG. 4. Least-squares fits to harmonic temperature and charge responses of PVF_2, for a heater-voltage frequency of 0.05 Hz.

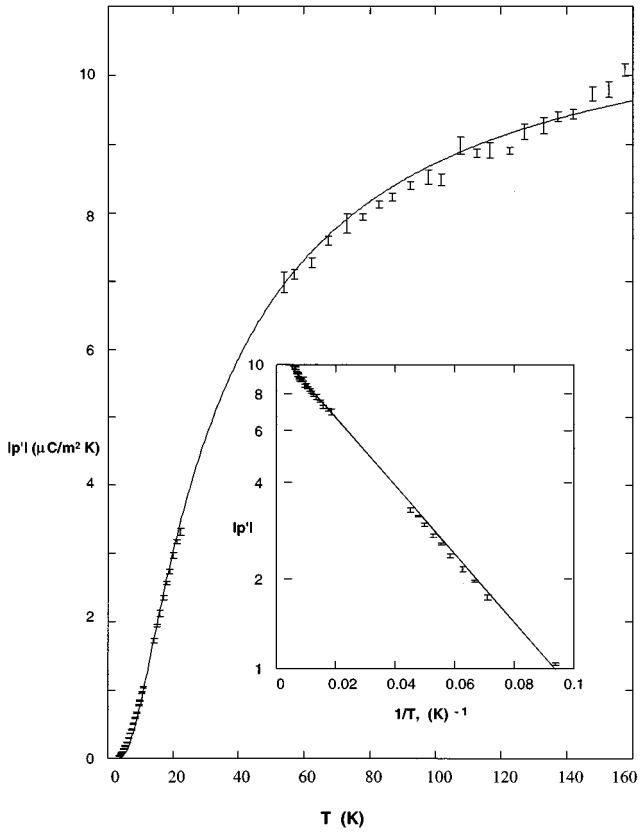

FIG. 5. Data averages plotted for p' vs T, and log p' vs $1/T$. The straight line in the inset represents a linear least-squares fit to the raw data from 10 to 160 K. This fit yielded a slope of (25.9 ± 0.06) K. The solid curve in the linear plot represents the corresponding exponential function.

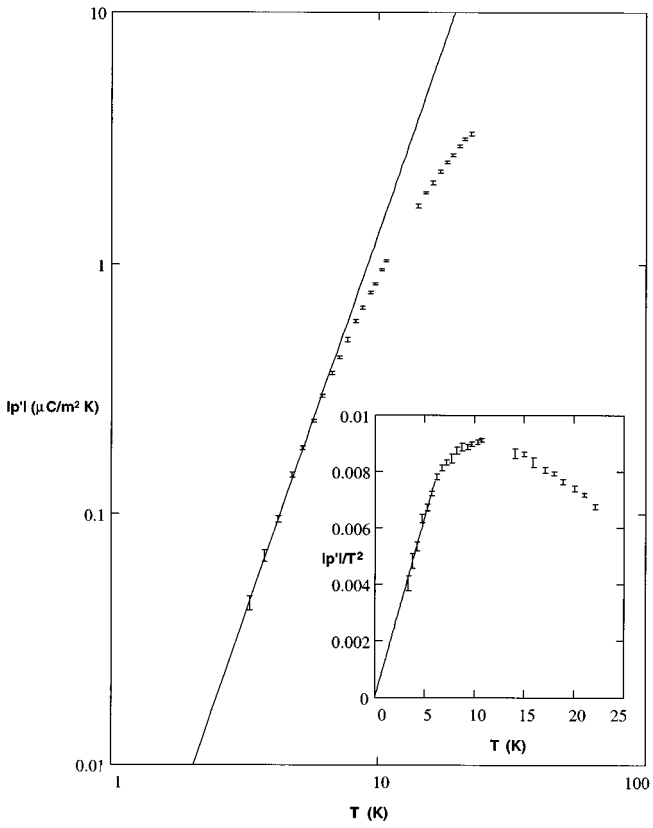

FIG. 6. Data averages of p' vs T, plotted with linear least-squares fits to the raw data on log-log scales. The length of each vertical error bar bounds the region of $\pm\overline{\sigma}$, where $\overline{\sigma}$ represents the root-mean-square standard deviation of the mean of approximately equal numbers of heating and cooling runs. The inset shows the same data plotted on linear scales, with $|p'|$ normalized by T^2.

An alternative explanation for this temperature dependence in Fig. 5 is that it reflects contributions from optical modes which remain dominant at low temperatures. The temperature dependence of such modes is characterized by Einstein functions, which are also exponential in temperature. These functions are often used to fit temperature-dependent measurements of p' and c_p for various substances,[5,45–49] although such data may sometimes be adequately explained by variations in the density of localized states.[50,51] Attempts at detailed fits to optic modes are often plagued with an excessive number of adjustable parameters, unless a few of the modes are dominant. This latter assumption is fortunately justified for studies of $LaNbO_3$ and $TiNbO_3$, because their neutron- and Raman-scattering data provide evidence for soft-mode enhancement of the amplitudes for a few optical phonons associated with structural phase transitions.[24,49] The amplitudes of the dominant optical modes are significantly enhanced at low temperature in these compounds as their frequencies approach zero (i.e., soft mode) (Ref. 24) in the vicinity of a displacive phase transition. Such transitions occur when two stable configurations separated by a potential barrier kT_c become unstable near the transition temperature T_c. Order-disorder transitions, on the other hand, have barrier heights much larger than kT_c, and therefore tunneling is dominant.[52]

There is, however, no evidence of any ''soft'' modes which might selectively enhance optical transitions in PVF_2 at low temperatures.[51,53,54] This indicates that thermal activation is a more plausible mechanism.

The effective temperature (25.9 ± 0.06) K of our two-parameter fit is intriguingly close to the condensation temperature of liquid hydrogen (i.e., 20.8 K), and is also in the temperature regime where we observe a rapid change in the magnitude of p'. There have often been conjectures that hydrogen bonds may be important in the ferroelectric characteristics exhibited by some substances near the condensation point of liquid hydrogen.[55] Although this exponential behavior of the pyroelectric coefficient is often found at low temperature in other substances, the activation temperatures deduced from the fits to the data are typically not close to 20.8 K, even when hydrogen is present.[45–47] This issue might be readily resolved for PVF_2 if it is feasible to make comparative measurements of p' with a deuterated sample, because the boiling point of deuterium is approximately 3 K above that of hydrogen at atmospheric pressure.

C. Low-temperature range from 3 to 23 K

The data in Fig. 6 show a distinct T^3 dependence for p' from 3 to ~ 6 K. The linear least-squares fit from the log-log plot yields an exponent of 3.07 ± 0.04 over this temperature range. This fit is not significantly improved by the addition of a linear term, predicted initially by Born[7] and subse-

quently by Grout and co-workers[8,9] for p_I. Note that a T^3 dependence for p' is consistent with the Szigeti prediction[11,12] for p_I, and with the expected temperature dependence of p_{II} for a crystalline polymer in the Debye limit.[26] The data from 6 to 23 K are not as well fit by a straight line, but a similar least-squares fit yields a slope of 1.95 ± 0.08.

The linear plot of p'/T^2 versus T, in the inset of Fig. 6, provides additional insight into the temperature dependence of p' at low temperature. The straight-line fit through the data from 3 to 6 K confirm the cubic temperature dependence of p' there. The fact that the extrapolated line intersects the origin is also consistent with the absence of significant contributions from either T^2- or T^1-dependent terms. In the region above 6 K, however, the short temperature interval of approximately zero slope, followed by the extended region of negative slope, are consistent with dominant contributions from T^2 and T^1 terms, respectively. As previously noted, the data in this transition region are also not well fit by the exponential function, successfully used at higher temperatures. In spite of its apparent complexity, this transition region merits further study because the relative amounts of p_I and p_{II} might be inferred from measurements of p' if α and c_p are measured well there.

The temperature dependence of p' displayed in Fig. 6 is consistent with the generic behavior of low-temperature measurements for the related parameters c_p and α for some other polymers. For example, the specific heat c_p for both amorphous and crystalline polyethylene CH_2 is reported to be cubic from 1 to 6 K, followed by T^2 and T^1 dependences at higher temperatures.[56] A similar behavior has also been observed for α in the vicinity of 6 K for many polymers classified as epoxy resins.[26] This indicates that the close packing of polymer strands at very low temperatures often facilitates enough phonon coupling between strands to successfully mimic a three-dimensional Debye medium.

IV. SUMMARY AND CONCLUSIONS

Our measurements from 3 to 307 K show several distinctive characteristics. The most remarkable is the T^3 dependence from 3 to 6 K. This is consistent with the prediction of Szigeti[11,12] for the primary contribution to the pyroelectric coefficient p_I, and with the Debye limit for the secondary contribution p_{II}.[15,26] In the range from 20 to 150 K, where the change in p' is largest, the data are readily fit by an exponential $(a_o)e^{-\theta/T}$, indicating a thermally activated process. At higher temperatures, near the glass transition at $T \sim 200$ K, our measurements suggest the possible existence of thermally driven hysteresis.

The data at intermediate temperatures from ~ 100 to ~ 250 K show an approximately constant value for the ratio of $|p'|/\alpha$.[26] This is consistent with a dominance of secondary pyroelectric effects, associated with thermal expansion of the sample in that temperature regime.

The area of potentially greatest interest, which is likely to yield most information about the internal interactions in PVF_2, is where the temperature dependence of p' deviates from α and c_p. Such deviations occur below ~ 60 K, where the magnitude of p' decreases rapidly with decreasing temperature. So far there is little data on α and c_p at low temperatures for PVF_2, and there is an obvious need to extend their range and accuracy there.[26,27]

ACKNOWLEDGMENTS

The generous help of W. Henderson is gratefully acknowledged. Special thanks are also due to J. I. Scheinbeim, B. A. Newman, and S. Esayan for helpful discussions about their work in this field. This work was supported by Grant No. NSF-DMR9401561.

[1] L. F. Hu, K. Takahashi, R. E. Salomon, and M. M. Labes, J. Appl. Phys. **50**, 2910 (1979).
[2] S. B. Lang, J. Appl. Phys. **50**, 5554 (1979).
[3] A. M. Glass and T. J. Negran, J. Appl. Phys. **50**, 5557 (1979).
[4] G. Teyssèdre, A. Bernès, and C. Lacabanne, Ferroelectrics **160**, 67 (1994).
[5] G.-R. Li and H. Ohigashi, Jpn. J. Appl. Phys. **31**, 2495 (1992).
[6] G. Teyssèdre and C. Lacabanne, Ferroelectrics **171**, 125 (1995).
[7] M. Born, Rev. Mod. Phys. **17**, 245 (1945).
[8] P. J. Grout, N. H. March, and T. L. Thorp, J. Phys. C **8**, 2167 (1975).
[9] P. J. Grout and N. H. March, Phys. Rev. Lett. **37**, 791 (1976).
[10] M. Born and K. Huang, *The Dynamical Theory of Crystal Lattices* (Clarendon, Oxford, 1954).
[11] B. Szigeti, Phys. Rev. Lett. **35**, 1532 (1975).
[12] B. Szigeti, Phys. Rev. Lett. **37**, 792 (1976).
[13] R. Radebaugh, Phys. Rev. Lett. **40**, 572 (1978).
[14] A. R. Blythe, *Electrical Properties of Polymers* (Cambridge University Press, London, 1979).
[15] H. S. Nalwa, *Ferroelectric Polymers—Chemistry, Physics, and Applications* (Marcel Dekker, New York, 1995).
[16] R. G. Kepler and R. A. Anderson, Adv. Phys. **41**, 1 (1992).
[17] R. W. Whatmore, Rep. Prog. Phys. **49**, 1335 (1986).
[18] A. J. Lovinger, Science **220**, 1115 (1983).
[19] H. Kawai, Jpn. J. Appl. Phys. **8**, 975 (1969).
[20] S. B. Lang, *Sourcebook of Pyroelectricity* (Gordon and Breach, New York, 1974).
[21] M. E. Lines and A. M. Glass, *Principles and Applications of Ferroelectric and Related Materials* (Clarendon, Oxford, 1977).
[22] C.-Z. Wang, R. Yu, and H. Krakauer, Phys. Rev. B **54**, 11 161 (1996).
[23] H. Dvey-Aharon and P. L. Taylor, Ferroelectrics **33**, 103 (1981).
[24] A. M. Glass and M. E. Lines, Phys. Rev. B **13**, 180 (1976).
[25] G. Heiland and H. Ibach, Solid State Commun. **4**, 353 (1966).
[26] G. Hartwig, *Polymer Properties at Room and Cryogenic Temperatures* (Plenum, New York, 1994).
[27] W. K. Lee and C. L. Choy, J. Polym. Sci. **13**, 619 (1975).
[28] C. S. Lynch and R. M. McMecking, Ferroelectrics **160**, 177 (1994).
[29] R. G. Kepler and R. A. Anderson, J. Appl. Phys. **49**, 4490 (1978).
[30] R. G. Kepler, R. A. Anderson, and R. R. Lagasse, Phys. Rev. Lett. **48**, 1274 (1982).

[31] R. Al-Jishi and P. L. Taylor, J. Appl. Phys. **57**, 902 (1985).
[32] M. G. Broadhurst, Bull. Am. Phys. Soc. **30**, 386 (1985).
[33] Uncertainties are largest at their extremes of the time evolution curves: near $t=0$, the rapid changes in temperature increase sampling noise, while at the longest times when the temperature nears saturation the signal-to-noise ratio is reduced because the pyroelectric response vanishes. These uncertainties were reduced by excluding data for which the linear correlation coefficient of the charge vs temperature fell below 0.995. The results were also excluded whenever less than four data points fell within the selected temperature interval.
[34] V. F. Kosorotov, L. S. Kremenchugskij, L. V. Levash, and L. V. Shchedrina, Ferroelectrics **160**, 125 (1994).
[35] A. van der Ziel, J. Appl. Phys. **44**, 546 (1973).
[36] H. Wang, Q. M. Zhang, L. E. Cross, and A. O. Sykes, Ferroelectrics **150**, 255 (1993).
[37] J. D. Zook and S. T. Liu, J. Appl. Phys. **49**, 4604 (1978).
[38] C. L. Choy, F. C. Chen, and K. Young, J. Polym. Sci. **19**, 335 (1981).
[39] D. K. Davies, in *Electrical Properties of Polymers*, edited by D. A. Seanor (Academic, New York, 1982).
[40] J. van Turnhout, in *Electrets*, edited by G. M. Sessler, Topics in Applied Physics, Vol. 33 (Springer-Verlag, Berlin, 1987).
[41] C. Dias, M. Simon, R. Quad, and D. K. Das-Gupta, J. Appl. Phys. D **26**, 106 (1993).
[42] J. I. Scheinbeim, K. T. Chung, K. D. Pae, and B. A. Newman, J. Appl. Phys. **51**, 5106 (1980).
[43] H. Burkard and G. Pfister, J. Appl. Phys. **45**, 3360 (1974).
[44] Y. Wada, Ferroelectrics **57**, 343 (1984).
[45] C. de la Heras, J. A. Gonzalo, and S. Vierira, Ferroelectrics **33**, 13 (1981).
[46] S. Vierira, C. de la Heras, and J. A. Gonzalo, Solid State Commun. **31**, 175 (1979).
[47] S. Vierira, C. de la Heras, and J. A. Gonzalo, Phys. Rev. Lett. **41**, 1822 (1978).
[48] J. Mangin and A. Hadni, Phys. Rev. B **18**, 7139 (1978).
[49] M. E. Lines and A. M. Glass, Phys. Rev. Lett. **39**, 1362 (1977).
[50] G. Burns, Solid State Commun. **35**, 811 (1980).
[51] M. Kobayashi, K. Tashiro, and H. Tadokoro, Macromolecules **8**, 158 (1975).
[52] *Structural Phase Transitions I*, edited by K. A. Müller and H. Thomas, Topics in Current Physics Vol. 23 (Springer-Verlag, Berlin, 1981).
[53] J. F. Legrand, B. Frick, B. Mourer, V. H. Schmidt, M. Bee, and J. Lajzerowicz, Ferroelectrics **109**, 321 (1990).
[54] G. L. Cessac and J. G. Curro, J. Polymer Sci. **12**, 695 (1974).
[55] V. K. Novik, A. M. Kousainov, A. B. Esengaliev, N. D. Gavrilova, and V. N. Novikov, Ferroelectrics **170**, 37 (1995).
[56] B. Wunderlich, J. Chem. Phys. **37**, 1203 (1962).